The Instability In Chiral Magnetohydrodynamics

Shuai Wang and Xu-Guang Huang

Fudan University

2024 年 12 月 8 日

USTC - Particle and Nuclear Physics

NPMW Mini Workshop

中国科学技术大学核物理系列小型研讨会

USTC-PNP-Nuclear Physics Mini Workshop

Outline

1. Background
   - Plasma,Alfvén Wave,...
   - Chiral Plasma
2. Chiral Anomaly
   - Chiral Hydrodynamics
   - Chiral Alfvén Wave
   - Chiral Plasma Instability
   - Chiral Magntovortical Instability
3. Summary and Outlook

Plasma

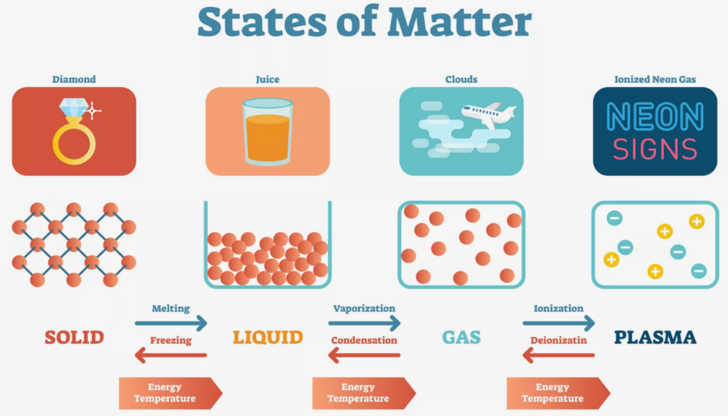

图 1: States of Matter [1]

[1] Helmenstine,Anne Marie,Ph.D."What Are the States of Matter?"ThoughtCo, Jun.7,2024.

Alfvén Wave

Considering ideal-MHD, one obtains the known MHD waves - **Alfvén wave** in incompressible fluid by *Alfvén,H.(1942)*.

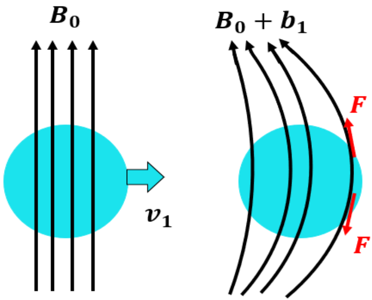

图 2: Alfvén wave

Dispersion relation:

$$\omega = \frac{\boldsymbol{B}_0 \cdot \boldsymbol{k}}{\sqrt{\mu_0 \rho}} \tag{1}$$

blue ball-fluid element with velocity $\boldsymbol{v}_1$, black lines-magnetic lines $\boldsymbol{B} = \boldsymbol{B}_0 + \boldsymbol{b}_1$, $\boldsymbol{B}_0$-background field, $\boldsymbol{b}_1, \boldsymbol{v}_1$- perturbations($\boldsymbol{B}_0 \perp \boldsymbol{b}_1, \boldsymbol{v}_1$), μ_0-vacuum magnetic permeability, ρ-mass density.

Accretion disks

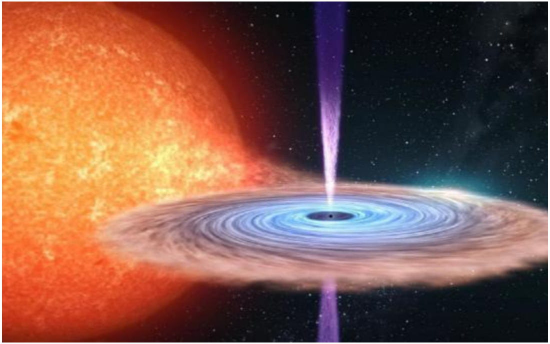

图 3: An artistic figure of the accretion disks

Most accretion disks probably transport angular momentum by magneto-hydrodynamic processes which is called **magnetorotational instability (MRI)** . It explains how a conducting fluid in differential rotation subjected to a magnetic field can be destabilized. *S.A.Balbus and J.F.Hawley(1991)*.

Chiral Plasma

The relativistic heavy ion collision experiments show that the quark gluon plasma (QGP) is in **strong magnetic fields** and **fluid vortical fields** .

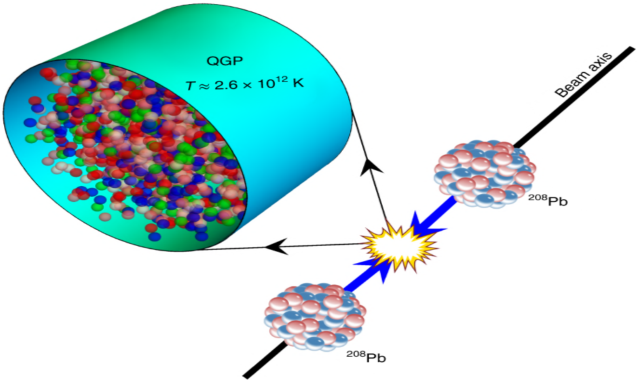

图 4: Schematic representation of a ^{208}Pb-^{208}Pb collision at the LHC.

Chiral Plasma

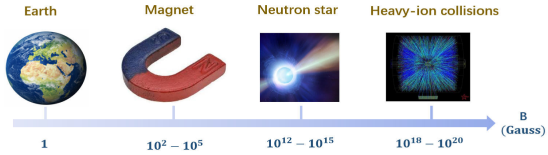

图 5: The magnetic field strength for different physical systems

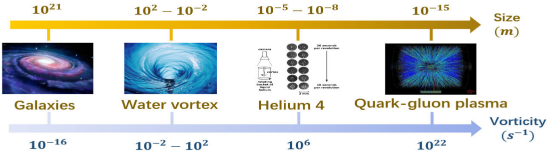

图 6: The vorticity in fluid systems at different scales

Chiral Anomaly and Anomalous Transport

Generally, a symmetry of a classical theory is also a symmetry of the quantum theory. However, if it is not, we call the symmetry "Anomaly". Here we focus on the **Chiral Anomaly**

$$\partial_\mu j_5^\mu = -\frac{e^2}{16\pi^2}\epsilon^{\mu\nu\alpha\beta}F_{\mu\nu}F_{\alpha\beta} \tag{2}$$

the axial current j_5^μ is not conserved for chiral fermions with $m = 0$. *"Adler,Bell and Jackiw(1969) or Fujikawa(1979)"* .

Anomalous phenomena, the **chiral separation effect(CSE)** and the **chiral magnetic effect(CME)** *"A.Vilenkin(1980); K.Fukushima et al.(2008), ..."*

$$\boldsymbol{j}_5 = \frac{\mu_V e^2}{2\pi^2}\boldsymbol{B} \qquad \boldsymbol{j}_V = \frac{\mu_5 e^2}{2\pi^2}\boldsymbol{B} \tag{3}$$

also the **chiral vortical effect(CVE)** are *"A.Vilenkin(1980), ..."*

$$\boldsymbol{j}_V = \frac{\mu_V\mu_5}{\pi^2}\boldsymbol{\omega} \qquad \boldsymbol{j}_5 = (\frac{T^2}{6} + \frac{\mu_V^2+\mu_5^2}{2\pi^2})\boldsymbol{\omega} \tag{4}$$

Chiral Hydrodynamics

The **Chiral Hydrodynamics (CHD)** was pioneered by *"D.T.Son and P.Surowka(2009)"*. Considering the CHD for right-handed chiral fermions in external electromagnetic fields

$$\partial_\mu T^{\mu\nu} = F^{\nu\lambda} j_\lambda \tag{5}$$

$$\partial_\mu j^\mu = C E^\mu B_\mu \tag{6}$$

here $T^{\mu\nu}$ is the energy-momentum tensor, j^μ is right-handed current, $E^\mu = F^{\mu\nu} u_\nu, B^\mu = \frac{1}{2}\epsilon^{\mu\nu\alpha\beta} u_\nu F_{\alpha\beta}$ are defined in the fluid rest frame, C is anomaly coefficient. In the Landau-Lifshitz frame *(1959)*

$$T^{\mu\nu} = (\epsilon + P) u^\mu u^\nu - P g^{\mu\nu} + \tau^{\mu\nu} \tag{7}$$

$$j^\mu = n u^\mu + V^\mu \tag{8}$$

with dissipative terms $\tau^{\mu\nu} u_\nu = V^\mu u_\mu = 0$.

Chiral Hydrodynamics

And the entropy current analysis

$$s^{\mu} = su^{\mu} + s_1^{\mu} \tag{9}$$

thus the 2nd law of thermodynamics tells us $\partial_\mu s^\mu \geq 0$

$$\partial_\mu s^{\mu} = \frac{\tau^{\mu\nu}\partial_\mu u_\nu}{T} - V^{\mu}[\partial_\mu(\frac{\mu}{T}) + \frac{E_\mu}{T}] - \boldsymbol{\frac{\mu}{T} C E^{\mu} B_{\mu}} + \partial_\mu[\frac{\mu}{T}V^{\mu} + s_1^{\mu}] \geq 0 \tag{10}$$

with projection operator-$\Delta^{\mu\nu} = g^{\mu\nu} - u^{\mu}u^{\nu}$, so

$$V^{\mu} = -T\sigma\Delta^{\mu\nu}\partial_\nu(\frac{\mu}{T}) + \sigma E^{\mu} + \boldsymbol{\xi_\omega \omega^{\mu}} + \boldsymbol{\xi_B B^{\mu}} \tag{11}$$

two new transport coefficients: ξ_ω-CVE and ξ_B-CME.

Chiral Alfvén Wave-CAW

Taking non-relativistic limit $|\boldsymbol{v}| \ll 1$, here $\boldsymbol{B}_0$ is a background field .

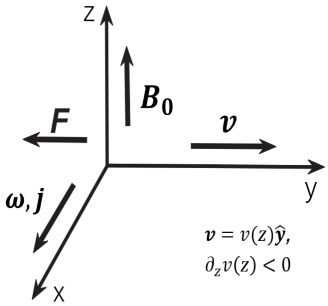

图 7: chiral Alfvén wave

$$(\epsilon + P)\partial_t \boldsymbol{v} = \xi_\omega \boldsymbol{\omega} \times \boldsymbol{B}_0 \quad (12)$$

dispersion relation

$$\omega = -\frac{\xi_\omega B_0}{\epsilon + P} k_z \quad (13)$$

The **Chiral Alfvén Wave (CAW)**. *N.Yamamoto(2015)*. Here the CVE induces a **Lorentz force** which acts as a restoring froce.

Dynamical electromagnetic field

Nonrelativistic limit $|\boldsymbol{v}| \ll 1$,power counting :
$\partial_t \sim \mathcal{O}(\epsilon_t)$,$\boldsymbol{\nabla} \sim \mathcal{O}(\epsilon_s)$,$\boldsymbol{v}, \boldsymbol{b} \sim \mathcal{O}(\delta)$, $\epsilon_s, \epsilon_t \ll 1$, $\delta \ll 1$, the conductivity σ is large enough, $n\boldsymbol{v} = (\boldsymbol{\nabla} \cdot \boldsymbol{E})\boldsymbol{v} \ll \sigma \boldsymbol{E}$, also $n\boldsymbol{E}$, assuming P, ϵ are constants, $\eta_s = 0$, then keeping $\boldsymbol{v} \sim \mathcal{O}(\delta)$

$$\begin{aligned} (\epsilon + P)\partial_t \boldsymbol{v} &\approx \boldsymbol{j} \times \boldsymbol{B} \\ \boldsymbol{j} &\approx \sigma(\boldsymbol{E} + \boldsymbol{v} \times \boldsymbol{B}) + \xi_B \boldsymbol{B} + \xi_\omega \boldsymbol{\omega} \\ \nabla \cdot \boldsymbol{v} &= 0 \\ \nabla \times \boldsymbol{B} \approx \boldsymbol{j} \quad \nabla \times \boldsymbol{E} &= -\partial_t \boldsymbol{B} \quad \nabla \cdot \boldsymbol{B} = 0 \end{aligned} \tag{14}$$

also the vector current conservation and axial current equation

$$\partial_t n + \boldsymbol{\nabla} \cdot \boldsymbol{j} = 0, \quad \boldsymbol{j} = n\boldsymbol{v} + \xi_\omega \boldsymbol{\omega} + \xi_B \boldsymbol{B} + \sigma(\boldsymbol{E} + \boldsymbol{v} \times \boldsymbol{B}) \tag{15}$$

$$\partial_t n_5 + \boldsymbol{\nabla} \cdot \boldsymbol{j}_5 = C_5 \boldsymbol{E} \cdot \boldsymbol{B}, \quad \boldsymbol{j}_5 = n_5 \boldsymbol{v} + \kappa_\omega \boldsymbol{\omega} + \kappa_B \boldsymbol{B} \tag{16}$$

Chiral Plasma Instability-CPI

$\boldsymbol{B} = \boldsymbol{B}_0 + \boldsymbol{b} = B_0\hat{\boldsymbol{z}} + \boldsymbol{b}$ $(\boldsymbol{b} \sim \mathcal{O}(\delta)), \boldsymbol{B}_0 \cdot \boldsymbol{b} = 0$, also $\boldsymbol{B}_0 \cdot \boldsymbol{v} = 0$

$$(\epsilon + P)\partial_t \boldsymbol{v} = (\boldsymbol{B}_0 \cdot \nabla)\boldsymbol{b} - \nabla(\boldsymbol{B}_0 \cdot \boldsymbol{b}) \tag{17}$$

$$\partial_t \boldsymbol{b} = (\boldsymbol{B}_0 \cdot \nabla)\boldsymbol{v} + \eta\nabla^2 \boldsymbol{b} + \eta\xi_B \nabla \times \boldsymbol{b} - \eta\xi_\omega \nabla^2 \boldsymbol{v} \tag{18}$$

here $\eta = 1/\sigma$ is resistivity. We first check the CME term ξ_B

$$\omega = \frac{1}{2}[-i\eta k_3(k_3 - \lambda\xi_B) \pm |k_3|\sqrt{-\eta^2(k_3 - \lambda\xi_B)^2 + \frac{4B_0^2}{\epsilon + P}}] \quad (\lambda = \pm 1) \tag{19}$$

here $\boldsymbol{k} \times \boldsymbol{b} \neq 0, i\eta\xi_B(\boldsymbol{k} \times \boldsymbol{b})_3 = 0$ and $\boldsymbol{k} \cdot \boldsymbol{b} = 0$ which limits $\boldsymbol{k} = (0, 0, k_3)$. The instability appears in a finite intervals $|k_3| \in (0, \xi_B)$- **Chiral Plasma Instability (CPI)** [2].

[2] Y.Akamatsu and N.Yamamoto,PRL.111,052002(2013)

Chiral Plasma Instability-CPI

What is the fate of chiral plasma instabilities above? Let's first recall the relation of triangle anomalies

$$\partial_t n_5 = C_5 \boldsymbol{E} \cdot \boldsymbol{B} \tag{20}$$

then one can integrate in all space

$$V\chi_5 \partial_t \mu_5 = C_5 \int d^3 \boldsymbol{x} \boldsymbol{E} \cdot \boldsymbol{B} = -\frac{C}{2} \int d^3 \boldsymbol{x} \boldsymbol{A} \cdot \boldsymbol{B} = -\frac{C}{2} \partial_t \mathcal{H}(t) \tag{21}$$

where we have assumed a homogeneity of the system, $n_5 = \chi_5 \mu_5(t)$, $\chi_5 \propto T^2$, χ_5 is the chiral susceptibility. And $\mathcal{H}$ is the Chern-Simons number (which is also called the magnetic helicity in plasma physics). The CPI once happens, however, the fermionic helicity will deplete.

Topology Property of CPI

Magnetic helicity is a fundamental quantity of magnetohydrodynamics that carries topological information about the magnetic field.

$$\mathcal{H} = \sum_{i=1}^{N} \mathcal{S}_i \phi_i^2 + 2 \sum_{i,j=1}^{N} \mathcal{L}_{ij} \phi_i \phi_j \tag{22}$$

where $\mathcal{S}_i$ is the Calugareanu-White self-linking number, and $\mathcal{L}_{ij}$ is the Gauss linking number.

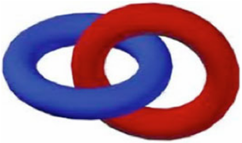

图 8: Magnetic helicity of two linked flux

$$\mathcal{H} = \int_V \boldsymbol{A} \cdot \boldsymbol{B} = \pm 2 \phi \phi \tag{23}$$

here $\mathcal{L} = \pm 1$

Topology Property of CPI

Linking number

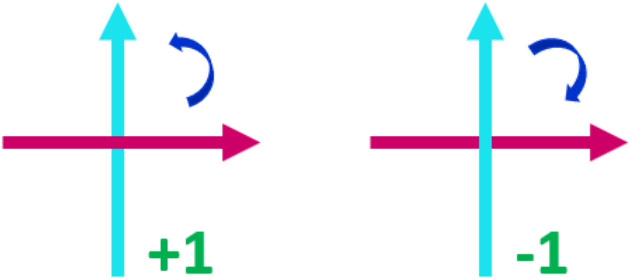

图 9: The sign of cross point

Topology Property of CPI

examples

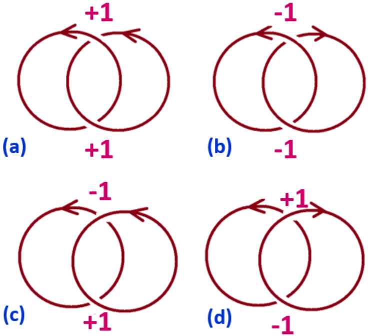

图 10: The simple linking number

so the linking numbers are $\mathcal{L}_{(a)} = \frac{1}{2}(1+1) = 1$, $\mathcal{L}_{(b)} = \frac{1}{2}(-1-1) = -1$ and $\mathcal{L}_{(c)}, \mathcal{L}_{(d)} = 0$.

Topology Property of CPI

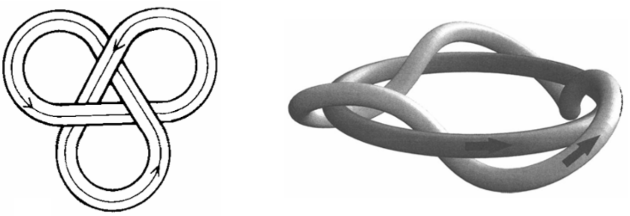

图 11: Linking number $= -3$

here the left one has magnetic helicity $\mathcal{H} = -3\phi^2$, and the right one has magnetic helicity $\mathcal{H} = -6\phi_1\phi_2$

Chiral Plasma Instability-CPI

An intuitive picture about the CPI

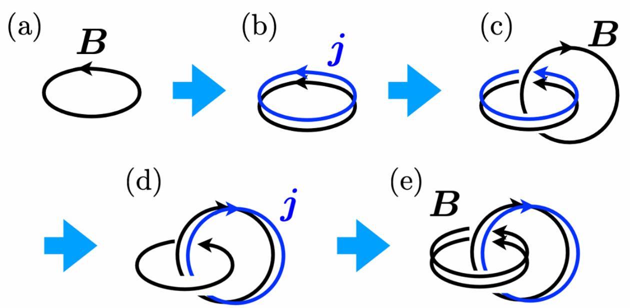

图 12: Intuitive picture of the CPI [3]

[3] arXiv:2305.01234

Chiral Magntovortical Instability-CMVI

now we focus on the CVE (setting $\xi_B = 0$)

$$\omega = \omega_\pm \equiv \frac{1}{2}[-i\eta \boldsymbol{k}^2 \pm \sqrt{\frac{4(\boldsymbol{B}_0\cdot\boldsymbol{k})^2}{\epsilon+P} - \eta^2\boldsymbol{k}^4 - i\cdot\eta\xi_\omega\boldsymbol{k}^2\frac{4(\boldsymbol{B}_0\cdot\boldsymbol{k})}{\epsilon+P}}] \quad (24)$$

$$\approx \pm \underbrace{\frac{(\boldsymbol{B}_0\cdot\boldsymbol{k})}{\sqrt{\epsilon+P}}}_{Alfven\ \ wave} - i\frac{\eta}{2}(1 \pm \frac{\xi_\omega}{\sqrt{\epsilon+P}})\boldsymbol{k}^2 \quad (25)$$

the instability occurs once $\xi_\omega > \sqrt{\epsilon+P}$ and applicable to any $|\boldsymbol{k}|$. Because the CVE and magnetic field are both included, we call this instability **Chiral Magnetovortical Instability (CMVI)** [4].

[4] S.Wang and XG.Huang,PRD 109,L121302(2024)

Chiral Magntovortical Instability-CMVI

An intuitive picture about the CMVI

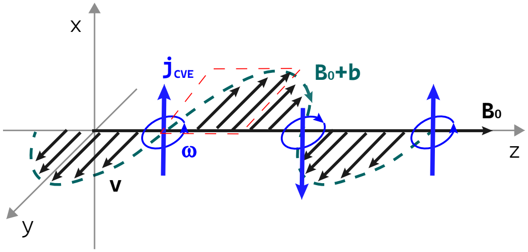

图 13: CMVI

The CVE currents induce new magnetic fields around themselves, the new magnetic fields will add the perturbed magnetic fields $\boldsymbol{b}$. If the CVE is strong enough to overcome the dissipative effects ($\xi_\omega > \sqrt{\epsilon + P}$), then $\boldsymbol{b}$ increases in red regions.

Chiral Magntovortical Instability-CMVI

One can integrate chiral anomaly equation and ignore the surface term

$$\partial_t(\int d^3\boldsymbol{x} j_5^0 + \frac{C_5}{2}\mathcal{H}_B) = 0 \tag{26}$$

where $j_5^0 = n_5 + \kappa_B \boldsymbol{v} \cdot \boldsymbol{B} + \kappa_\omega \boldsymbol{v} \cdot \boldsymbol{\omega}$. Next we introduce different helicities

$$\mathcal{H}_B \equiv \int d^3\boldsymbol{x}\boldsymbol{A} \cdot \boldsymbol{B} \qquad \mathcal{H}_5 \equiv \int d^3\boldsymbol{x}\, n_5 \tag{27}$$

$$\mathcal{H}_c \equiv \int d^3\boldsymbol{x}\boldsymbol{v} \cdot \boldsymbol{B} \qquad \mathcal{H}_v \equiv \int d^3\boldsymbol{x}\boldsymbol{v} \cdot \boldsymbol{\omega} \tag{28}$$

here $\mathcal{H}_{B/5/c/v}$ are magnetic,fermion,cross,fluid helicities. Therefore

$$\chi_5 \partial_t \mu_5 = -\frac{C_5}{2}\partial_t \bar{\mathcal{H}}_b - \kappa_B \partial_t \bar{\mathcal{H}}_c - \kappa_\omega \partial_t \bar{\mathcal{H}}_v - \Gamma \chi_5 \mu_5 \tag{29}$$

the notation $\Gamma(m)$ is the chirality relaxation rate in order to account for the chirality-flipping process due to mass, with $\Gamma(m=0)=0$.

Chiral Magntovortical Instability-CMVI

the average kinetic,magnetic energy and various helicities in helicity basis

$$\mathcal{E}_{\boldsymbol{v}}(t) = \frac{1}{2} < \boldsymbol{v}^2 >= \frac{1}{2V}\int_{\boldsymbol{k}}(|v_+|^2 + |v_-|^2), \qquad \mathcal{E}_{\boldsymbol{b}'}(t) = \{\boldsymbol{v} \to \boldsymbol{b}'\} \quad (30)$$

$$\bar{\mathcal{H}}_c(t) =< \boldsymbol{v} \cdot \boldsymbol{B} >= \frac{1}{V}\int_{\boldsymbol{k}}(v_+ b_+^* + v_- b_-^*) \quad (31)$$

$$\bar{\mathcal{H}}_{\boldsymbol{v}}(t) =< \boldsymbol{v} \cdot \boldsymbol{\omega} >= \frac{1}{V}\int_{\boldsymbol{k}} |\boldsymbol{k}| \cdot (|v_+|^2 - |v_-|^2) \quad (32)$$

$$\bar{\mathcal{H}}_b(t) =< \boldsymbol{A} \cdot \boldsymbol{B} >= \frac{1}{V}\int_{\boldsymbol{k}} \frac{1}{|\boldsymbol{k}|} \cdot (|b_+|^2 - |b_-|^2) \quad (33)$$

we have chosen an initial condition such that $\mathcal{H}_b(t=0) = \mathcal{H}_v(t=0) = 0$, which implies that they remain zero throughout the time evolution.

Chiral Magntovortical Instability-CMVI

Initial values: $\xi'_\omega = 5$, $|\boldsymbol{B}'_0| = 5$, $v_+(0) = b'(0) = \frac{0.1}{exp(10\eta|k_z|-100)+1}$. (lines in red/blue/purple/orange related to $\eta\Gamma = 0, 0.01, 0.02, 0.03.$)

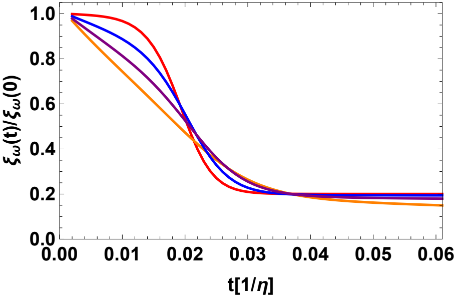

图 14: Evolution of ξ'_ω

- The CVE coefficient ξ'_ω decrease with time
- $\Gamma = 0$ means a pure Alfvén wave, so $\xi'_\omega = 1$ in final time
- $\Gamma \neq 0$, $\xi'_\omega(t) \to 0$ with time increases

Chiral Magntovortical Instability-CMVI

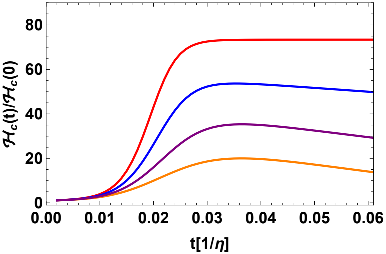

(a) Evolution of $\mathcal{H}_c$

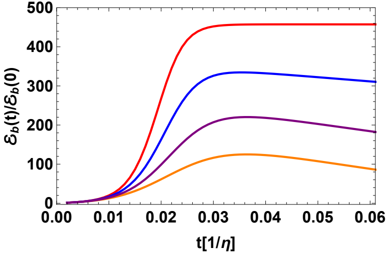

(b) Evolution of $\mathcal{E}_b$

图 15: the cross helicity $\mathcal{H}_c$ and magnetic energy $\mathcal{E}_b$

- $\mathcal{H}_c$ and $\mathcal{E}_b$ increase with time
- $\Gamma = 0$ means a pure Alfvén wave, $\mathcal{H}_c/\mathcal{E}_b$ are stationary finallly
- $\Gamma \neq 0$, $\mathcal{H}_c/\mathcal{E}_b \uparrow$ first, then $\downarrow$. The turning point satisfies $\xi'_\omega(t) = 1$
- $\mathcal{E}_b \uparrow$ means a dynamo effect, the magnification is 10-20

Summary and Outlook

1.CPI and CMVI

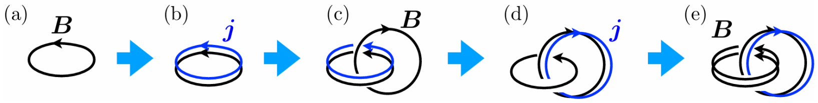

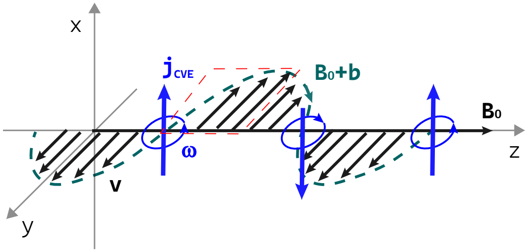

Summary and Outlook

2.the CMVI provides a mechanism by transferring chirality of constituent particles to the cross helicity of the system. Which expands the scope of the CME.

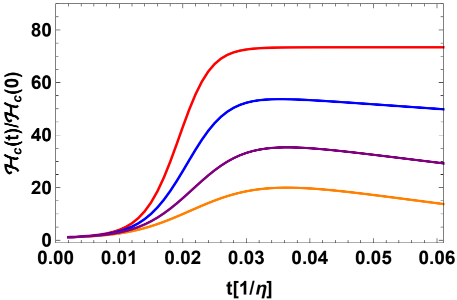

$$\omega = \pm \frac{(\boldsymbol{B}_0 \cdot \boldsymbol{k})}{\sqrt{\epsilon + P}} - i\frac{\eta}{2}(1 \pm \frac{\xi_\omega}{\sqrt{\epsilon + P}})\boldsymbol{k}^2$$

Summary and Outlook

3. All helicities are conserved $\partial_t \mathcal{H} = 0$

$$\mathcal{H}_B \equiv \int d^3\boldsymbol{x}\boldsymbol{A}\cdot\boldsymbol{B} \qquad \mathcal{H}_5 \equiv \int d^3\boldsymbol{x}\, n_5$$

$$\mathcal{H}_c \equiv \int d^3\boldsymbol{x}\boldsymbol{v}\cdot\boldsymbol{B} \qquad \mathcal{H}_v \equiv \int d^3\boldsymbol{x}\boldsymbol{v}\cdot\boldsymbol{\omega}$$

$$\mathcal{H} = \mathcal{H}_5 + \frac{C_5}{2}\mathcal{H}_B + \kappa_B\mathcal{H}_c + \kappa_\omega\mathcal{H}_v$$

It is interesting to include all helicities and explore the transformations between them, especially the vorticity, and the topological properties.

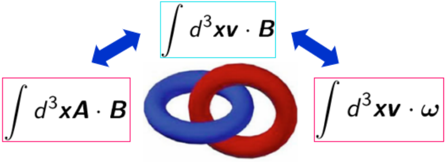

Summary and Outlook

4. We hope the CMVI can explain the magnetic field origin of the galaxies, stars, and planets in some points.

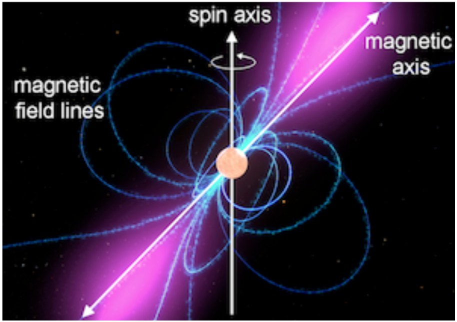

图 16: The neutron star with a strong magnetic field (blue lines)

Thank you for your attention!